Supporting Information

Conformations of Human Telomeric G-Quadruplex Studied Using a Nucleotide-Independent Nitroxide Label

Xiaojun Zhang,[†] Cui-Xia Xu,[‡] Rosa Di Felice,[§,∥] Jiri Sponer,[⊥,#] Barira Islam,[⊥] Petr Stadlbauer,[#] Yuan Ding,[†] Lingling Mao,[‡,@] Zong-Wan Mao,[‡] and Peter Z. Qin*[,†]

[†]Department of Chemistry, University of Southern California, Los Angeles, California 90089, United States

[‡]School of Chemistry and Chemical Engineering**,** Sun Yat-Sen University, Guangzhou, China

[§]Department of Physics and Astronomy, University of Southern California, Los Angeles, California 90089, United States

[∥]Center S3, CNR institute of Nanoscience, Modena, Italy

[⊥]Central European Institute of Technology (CEITEC), Masaryk University, Campus Bohunice, Kamenice 5, 625 00 Brno, Czech Republic

[#]Institute of Biophysics, Academy of Sciences of the Czech Republic, Kralovopolska 135, 612 65, Brno, Czech Republic

[@]Present address: Department of Chemistry, Northwestern University, Evanston, Illinois 60208, United States

*To whom correspondence should be addressed: LJS-251, 840 Downey Way, Los Angeles, California 90089-0744; Telephone: (213) 821-2461; Fax: (213) 740-0930; Email: pzq@usc.edu.

S.1. Molecular Dynamics Simulations

S.1.1. Methods

All-atom Molecular Dynamics (MD) simulations were carried out in explicit solvent using as starting structures coordinates of: (i) quadruplex A of crystal structure PDB entry 1KF1 (*1*) for parallel G-quadruplex (GQ); and (ii) model 1 of NMR structure, PDB entry 143D (*2*) for anti-parallel basket GQ. We used 0.15 M NaCl excess salt conditions for the MD simulations. The solvent molecules and additional ions for simulations were added using the xleap module of AMBER12. The water molecules and ions other than the channel cations were removed from the native PDBs in the starting structure. The channel K^+ ions in PDB entry 1KF1 were replaced with Na^+ ions for the present simulations. The system was first neutralized by Na^+ ions and then excess NaCl of 0.15 M concentration was added to the system. Water-model specific (SPC/E here) AMBER-adapted Joung and Cheatham parameters for Na^+ (radius 1.212 Å and well depth of 0.3526418 kcal mol^{-1}) and Cl^- ions (radius 2.711 and well depth 0.0127850) were used (*3*). Since we do not simulate transitions between different structures, it is sufficient to make the simulation using only one cation type, as the structural differences between NaCl and KCl simulations of a given GQ fold are small (for more discussion see (*4*)).

The system was solvated in the SPC/E water model and placed in a truncated octahedral box with a minimal distance of 10 Å of solute from the box border. The MD simulations were carried out with the Cornell *et al.* force field basic version parm99, with the bsc0 (*5*) and χ_{OL4} refinements (*6*). The bsc0 is essential to obtain stable DNA trajectories (*5*). χ_{OL4} has provided further structural improvement in simulations of GQs with *syn* guanosines as it improves the shape of the *syn* region and the *syn*/*anti* balance (*6, 7*). Both modules are standard and endorsed by the latest versions of AMBER code ambertools for DNA simulations.

The protocol for energy minimization and equilibration in explicit solvent was adopted from Stadlbauer *et al.* (*7*). Each system was first minimized with 500 steps of steepest descent followed by 500 steps of conjugate gradient minimization with 25 kcal mol^{-1} A^{-2} position restraints on DNA atoms. It was then heated from 0 to 300 K for 100 ps with constant volume and position restraints of 25 kcal mol^{-1} A^{-2}. Minimization with 5 kcal mol^{-1} A^{-2} restraints followed, using 500 steps of steepest descent method and 500 steps of conjugate gradient. The restraints of 5 kcal mol^{-1} A^{-2} were maintained on DNA atoms and the system was equilibrated for 50 ps at constant temperature of 300 K and pressure of 1 atm. An analogous series of alternating minimizations and equilibrations followed using decreasing position restraints of 4, 3, 2 and 1 kcal mol^{-1} A^{-2} consecutively. The final equilibration was carried out with position restraints of 0.5 kcal mol^{-1} A^{-2} and starting velocities from the previous equilibration, followed by a short free molecular dynamics simulation of 50 ps. Temperature and pressure coupling during equilibration was set to 0.2 and coupling during the last molecular dynamics phase was set to 5.

The final MD simulations were performed with the PMEMD CUDA version of AMBER12. Periodic boundary conditions were defined by the PME algorithm and the non-bonded cut-off was set to 9 Å. The SHAKE algorithm was used to constrain hydrogen atoms with a tolerance of 0.0001 Å and an integration time step of 2fs (*8*). The simulations were carried out at constant pressure of 1 atm and constant temperature of 300 K maintained using Berendsen weak coupling thermostat (*9*). The final production run without restraints was carried out for continuous 10 μs and the frames were written at every 10 ps.

For each of the resulting MD trajectory, snapshots at regular time intervals of every 10 ns were collected. These were used as input structures for modeling inter-nitroxide distances using the NASNOX program, following procedures described in the Methods section of the main text.

S.1.2. Additional MD data

S1.2.1. Inter-nitroxide distances predicted from MD trajectory obtained from PDB entry 1KF1 (parallel GQ).

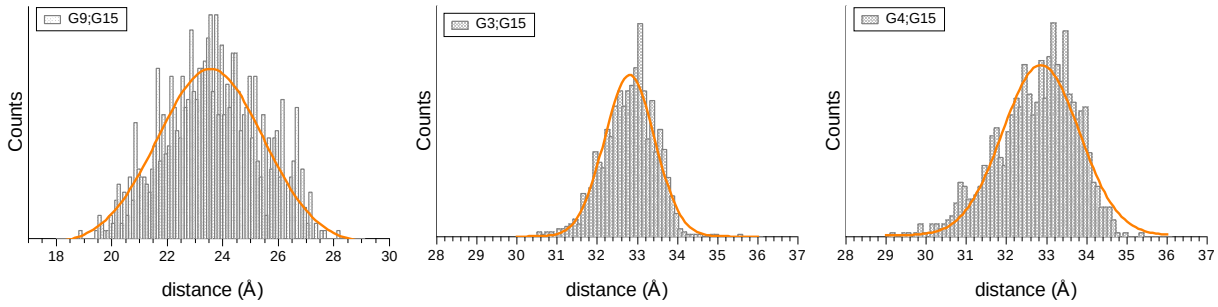

Figure S1: Histogram plots of the statistical distributions of the inter-spin distances in double labeled (G9;G15), (G3;G15) and (G4;G15) hTel-22 DNA. The three Gaussian fits (orange curves) have comparable accuracies and the predicted distances from the fits (peak center and standard deviation) are: 23.6±1.6 Å, 32.8±0.5 Å and 32.9±0.8 Å for (G9;G15), (G3;G15) and (G4;G15), respectively.

S1.2.2. Inter-nitroxide distances predicted from MD trajectory obtained from PDB entry 143D model 1 (antiparallel GQ).

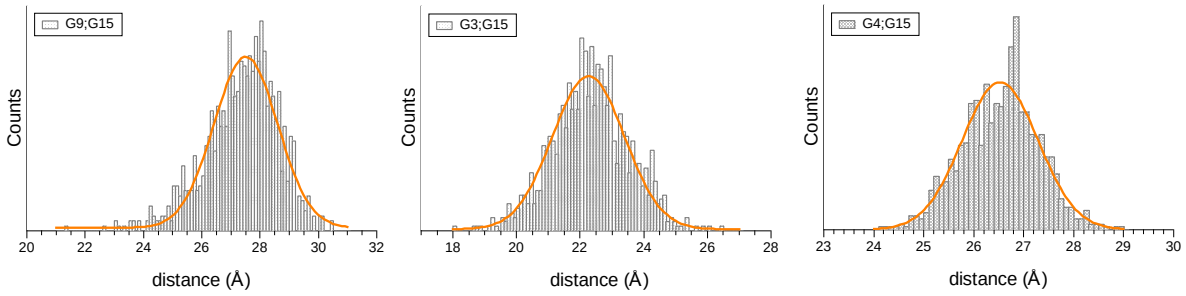

Figure S2: Histogram plots of the statistical distributions of the inter-spin distances in double-labeled (G9;G15), (G3;G15) and (G4;G15) hTel-22 DNA. The three Gaussian fits (orange curves) have comparable accuracies and the predicted distances from the fits (peak center and standard deviation) are: 27.5±0.9 Å, 22.3±1.0 Å and 26.5±0.7 Å for (G9;G15), (G3;G15) and (G4;G15), respectively.

S1.2.3. Analyses of all inter-R5 distances.

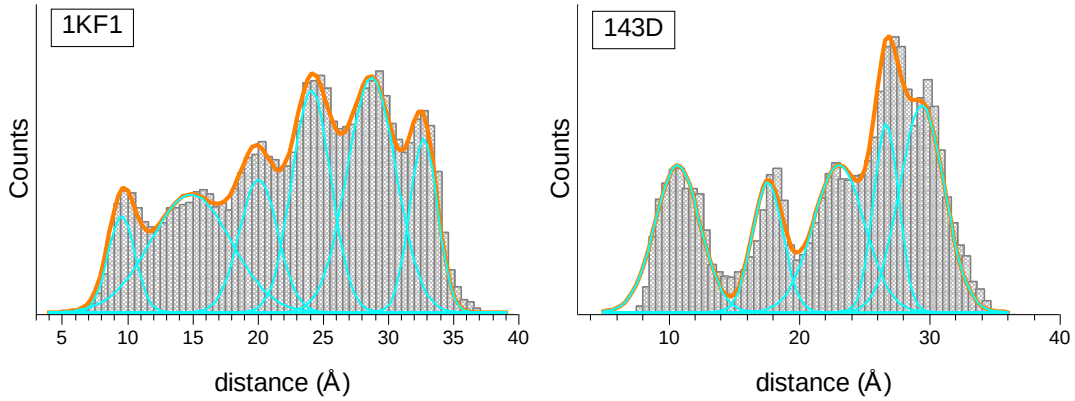

Figure S3: Distribution of all inter-R5 distances, computed with the program NASNOX from the MD trajectories of 1KF1 (left) and 143D (right) over 10 µs. The results of multi-Gaussian fits are collected in Table S1. Note that the predicted distance of set (G9;G15): 22.9 Å in 1KF1 and 27.7 Å in 143D, belongs to the 4th peak in 1KF1 and 4th peak in 143D. Each of them is one of the narrower distributions in respective profile.

Table S1: Peak center and standard deviation (σ) for the multi-Gaussian fits illustrated in Figure S3.

peak #	center (Å)	σ (Å)
1KF1		
1	9.5	0.9
2	14.8	2.6
3	20.0	1.2
4	24.1	1.3
5	28.7	1.6
6	32.7	0.9
143D		
1	10.7	1.5
2	17.6	1.0
3	23.0	1.7
4	26.7	0.8
5	29.4	1.5

S.2. DEER control

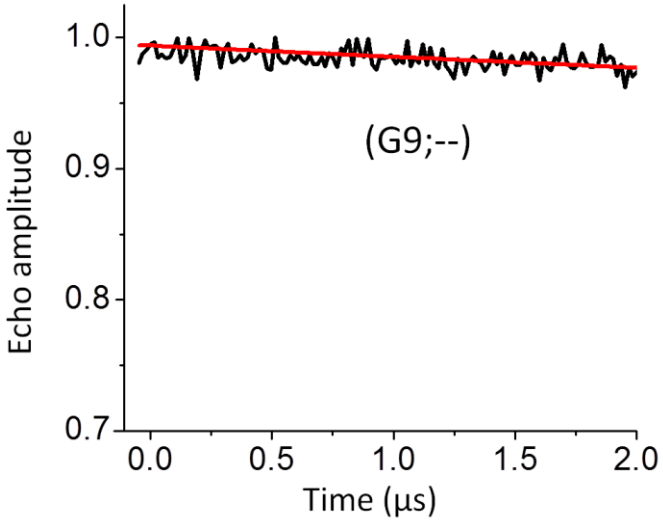

Figure S4: An example of DEER measurement on a single-labeled hTel-22. The spin label was attached to site G9, and the sample was designated as (G9; --). The black trace represents the measured echo decay, and the red trace represents the background computed by fitting an exponential decay corresponding to a homogeneous 3-dimentional distribution of electron spin to the last half of the data.

S.3. Additional NASNOX predicted distances

Table S2: Predicted inter-R5 distances for antiparallel (PDB entry 143D), parallel structure (PDB entry 1KF1), hybrid-1 (PDB entry 2HY9) and hybrid-2 (PDB entry 2JPZ) structures.

Data set[a]	Predicted distances (Å)			
	143D[b] (antiparallel)	1KF1 (parallel)	2HY9[c] (hybrid-1)	2JPZ[d] (hybrid-2)
(G9; G15)	27.7	22.9	28.9	12.0
(G3; G15)	21.7	30.6	26.4	30.3
(G4; G15)	24.0	29.9	29.1	30.3

[a]data set residue numbers are according to the hTel-22 sequence. The corresponding residue number for G3, G4, G9 and G15 are G5, G6, G11, and G17, respectively, in the 26-nt sequence for 2HY9 and 2JPZ.
[b]average of 6 NMR models
[c]average of 10 NMR models
[d]average of 10 NMR models

S.4. Additional DEER data analyses

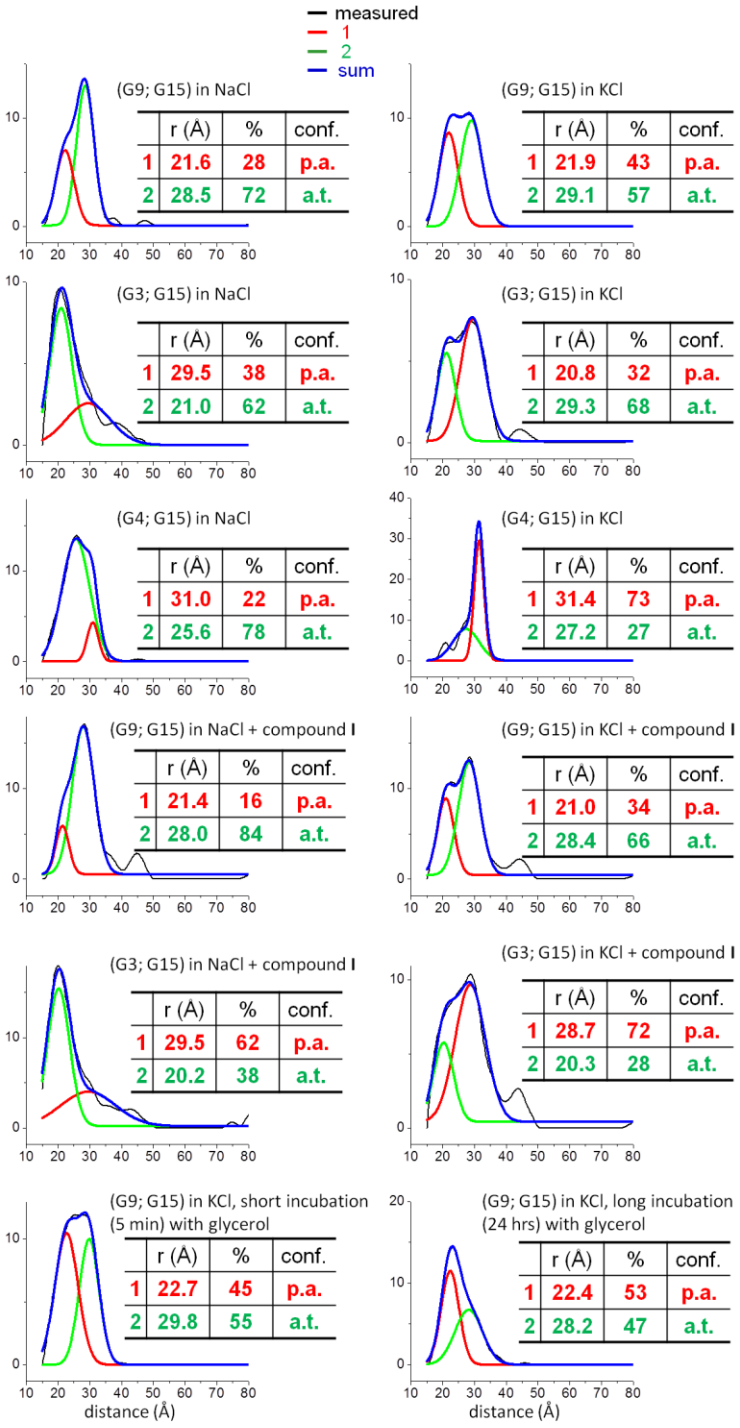

Figure S5: Two-Gaussian fit of DEER distance distribution profiles generated by Tikhonov regulation. Fitting was carried out following a reported approach (*10-13*), with the amplitude, center position, and width of each Gaussian function varied; and a $\chi 2$ metric calculated to identify the best fit. Tables in insets show the resulting center distance (r) and percentage (%) for each Gaussian, as well as the assignments of parallel (p.a.) or anti-parallel (a.t.) conformations.

S.5. Interactions between compound I and R5 labeled hTel-22

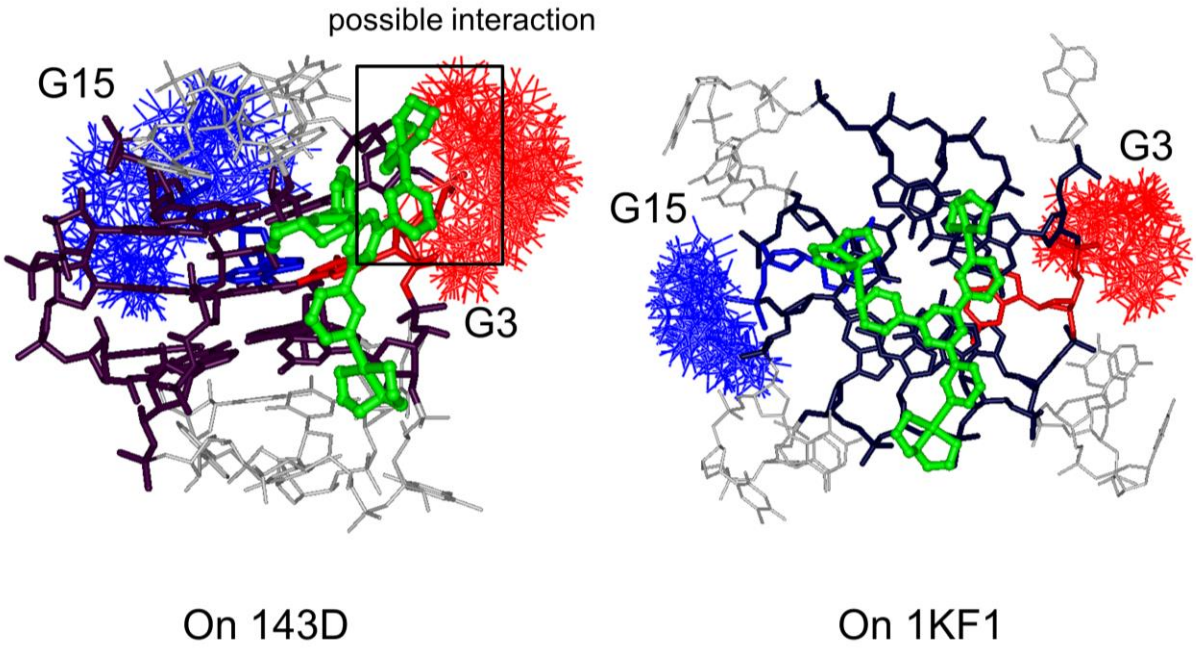

Figure S6: Molecular docking of compound **I** on PDB entries 143D (antiparallel GQ) and 1KF1 (parallel GQ) (*14*). The nucleotide G3 and its corresponding NASNOX predicted R5 rotamers are shown in red, and G15 and its R5 rotamers are shown in blue. The black box indicates the region where compound **I** and R5 rotamers on G3 may have crashed into each other.

References:

1. Parkinson, G. N., Lee, M. P., and Neidle, S. (2002) Crystal structure of parallel quadruplexes from human telomeric DNA, *Nature 417*, 876-880.
2. Wang, Y., and Patel, D. J. (1993) Solution structure of the human telomeric repeat d[AG3(T2AG3)3] G-tetraplex, *Structure 1*, 263-282.
3. Joung, I. S., and Cheatham, T. E., 3rd. (2008) Determination of alkali and halide monovalent ion parameters for use in explicitly solvated biomolecular simulations, *J Phys Chem B 112*, 9020-9041.
4. Sponer, J., Cang, X., and Cheatham, T. E., 3rd. (2012) Molecular dynamics simulations of G-DNA and perspectives on the simulation of nucleic acid structures, *Methods 57*, 25-39.
5. Perez, A., Marchan, I., Svozil, D., Sponer, J., Cheatham, T. E., 3rd, Laughton, C. A., and Orozco, M. (2007) Refinement of the AMBER force field for nucleic acids: improving the description of alpha/gamma conformers, *Biophys J 92*, 3817-3829.
6. Krepl, M., Zgarbova, M., Stadlbauer, P., Otyepka, M., Banas, P., Koca, J., Cheatham, T. E., 3rd, Jurecka, P., and Sponer, J. (2012) Reference simulations of noncanonical nucleic acids with different chi variants of the AMBER force field: quadruplex DNA, quadruplex RNA and Z-DNA, *J Chem Theory Comput 8*, 2506-2520.
7. Stadlbauer, P., Krepl, M., Cheatham, T. E., 3rd, Koca, J., and Sponer, J. (2013) Structural dynamics of possible late-stage intermediates in folding of quadruplex DNA studied by molecular simulations, *Nucleic Acids Res 41*, 7128-7143.
8. Ryckaert, J. P., Ciccotti, G., and Berendsen, H. J. C. (1977) Numerical-Integration of Cartesian Equations of Motion of a System with Constraints - Molecular-Dynamics of N-Alkanes, *Journal of Computational Physics 23*, 327-341.
9. Berendsen, H. J. C., Postma, J. P. M., Vangunsteren, W. F., Dinola, A., and Haak, J. R. (1984) Molecular-Dynamics with Coupling to an External Bath, *Journal of Chemical Physics 81*, 3684-3690.
10. Blackburn, M. E., Veloro, A. M., and Fanucci, G. E. (2009) Monitoring inhibitor-induced conformational population shifts in HIV-1 protease by pulsed EPR spectroscopy, *Biochemistry 48*, 8765-8767.
11. Galiano, L., Ding, F., Veloro, A. M., Blackburn, M. E., Simmerling, C., and Fanucci, G. E. (2009) Drug pressure selected mutations in HIV-1 protease alter flap conformations, *J Am Chem Soc 131*, 430-431.
12. Kear, J. L., Blackburn, M. E., Veloro, A. M., Dunn, B. M., and Fanucci, G. E. (2009) Subtype polymorphisms among HIV-1 protease variants confer altered flap conformations and flexibility, *J Am Chem Soc 131*, 14650-14651.
13. Casey, T. M., and Fanucci, G. E. (2015) Spin labeling and Double Electron-Electron Resonance (DEER) to Deconstruct Conformational Ensembles of HIV Protease, *Methods in Enzymology 564*, 153-187.
14. Xu, C.-X., Shen, Y., Hu, Q., Zheng, Y.-X., Cao, Q., Qin, P. Z., Zhao, Y., Ji, L.-N., and Mao, Z.-W. (2014) Stabilization of Human Telomeric G-Quadruplex and Inhibition of Telomerase Activity by Propeller-Shaped Trinuclear Pt(II) Complexes, *Chemistry – An Asian Journal 9*, 2519-2526.